A Neuronal Model for Visually Evoked Startle Responses in Schooling Fish

Master thesis

by
Andrej Warkentin
Bernstein Center for Computational Neuroscience - Berlin

Supervisors:
Dr. Pawel Romanczuk
Bernstein Center for Computational Neuroscience - Berlin
Prof. Dr. Henning Sprekeler
Technische Universität Berlin

Contents

Abstract

Many aspects of fish school behavior can be explained qualitatively by self-propelled agent models with social interaction forces that are based on either metric or topological neighborhoods. Recently, startling of fish has been analyzed in its dependence of the network structure (Rosenthal et al., 2015) but a mechanistic model and its influence on the collective behavior is missing. Here we couple a model for collective behavior with a neuronal model that receives looming visual stimulus input to initiate a startle response, inspired by the neurobiologically well-studied Mauthner cell system. First, we analyzed the basic properties of the startle behavior of a single fish as a reaction to a looming stimulus. On the group level, we looked at startling frequency as well as group cohesion and polarization depending on neuronal and collective behavior parameters via simulations of the combined model. Our results indicate that the startling frequency strongly depends on the dynamics of the group structure, e.g. when the group approaches a boundary of the arena. In summary, we took first steps towards a biologically plausible model for startle response initiation in the context of collective motion.

1. Introduction

- visual ecology
  - warning: making analogies to human vision is almost always misleading
  - "sensory world of each species is unique"
  - color vision in fish: Visual Ecology pp. 159
  - fish orient to overhead polarization orientation in laboratory Hawryshyn 1992
  - most fish species don't have a fovea (Encyclopedia of Fish Physiology, p. 141) so that eye movements/saccades should not be interpreted as fixations as is the case for humans
  - they do have different ganglion cell densities though, see Pita et al. (2015)
  - zebrafish have a row-ordered retinal mosaic with alternating rows with LWS double cones (red and green) and rows with SWS (blue and ultraviolet)
  - rhodopsin (based on vitamin A1, shorter, "blue" wavelengths) more in marine fish and porphyropsins (based on A2, longer, "green" wavelengths) rather in freshwater fish (more green environment)
  - important thing to remember: the visual field above a fish is very different from the lateral view which is again different from the visual field below a fish
  - fritsches and marshall 2002: eye movements in teleosts
  - here I cite Tytell and Lauder (2008)

2. Methods and Materials

2.1. Neuronal model

$$I(t) = f(\theta(t)) \tag{1}$$

$$\theta(t) = 2 \cdot \arctan(\frac{L/2}{distance}) \tag{2}$$

$$\tau_\rho \frac{d\rho}{dt} = -(\rho(t) - \rho_0) + c_\rho I(t) + \eta_\rho(t) \tag{3}$$

$$\tau_m \frac{dV_m}{dt} = -(V(t) - E_L) + R_m I(t) - \rho(t) + \eta_m(t) \tag{4}$$

2.2. Adiabatic approximation

We assume that the timescale of the Input is much higher that the timescale of the neuronal dynamics so that we have a the following stationary process:

$$\hat{V}_m(t) = E_L + I_{tot}(t) + noise \tag{5}$$

where

$$I_{tot}(t) = R_m I(t) - \hat{\rho}(t) \tag{6}$$

$$\hat{\rho}(t) = c_\rho 10^7 I(t) + \rho_0 \tag{7}$$

$$I(t) = 10^{-11} c_{exc} f(\theta(t)) = 10^{-11} c_{exc}(m \cdot \theta(t) + b) \tag{8}$$

We set all noise to zero and want to find the input at which the membrane potential reaches the threshold $V_t = -61$ mV:

$$\hat{V}_m(t) \stackrel{!}{=} V_t \tag{9}$$

$$\Leftrightarrow E_L + R_m I(t) - c_\rho I(t) - \rho_0 \stackrel{!}{=} V_t \tag{10}$$

Inserting values for the fixed parameters $E_L = -79$ mV, $R_m = 10$ MΩ and $V_t = -61$ mV:

$$-0.079 + 10^7 I(t) - c_\rho 10^7 I(t) - \rho_0 \stackrel{!}{=} -0.061 \tag{11}$$

$$10^7 I(t) - c_\rho 10^7 I(t) - \rho_0 \stackrel{!}{=} 0.018 \tag{12}$$

$$10^{-4} c_{exc} f(\theta(t))(1 - c_\rho) - \rho_0 \stackrel{!}{=} 0.018 \tag{13}$$

$$f(\theta(t)) \stackrel{!}{=} \frac{180 + \rho_0 10^4}{c_{exc}(1 - c_\rho)} \tag{14}$$

$$\theta(t) \stackrel{!}{=} \frac{180 + \rho_0 10^4}{m \cdot c_{exc}(1 - c_\rho)} - \frac{b}{m} \tag{15}$$

2.3. Further points

- first paragraph

3. Results

3.1. Response properties of a single LIF neuron

As a first step we presented a single LIF neuron with the visual angle θ over time as input current. In order to compare our results with experimental work (see e.g. Bhattacharyya et al. (2017), Temizer et al. (2015), Dunn et al. (2016)) we analyzed the angle, distance, latency and time-to-collision of the response. The response onset was defined as the time of the first spike of the LIF neuron. We ignore further processing time after the spike of the Mauthner cell because it is in the order of milliseconds (Preuss and Faber (2003)) and thus irrelevant with respect to the overall response time which is in the order of at least hundreds of milliseconds for visual stimuli (Preuss et al., 2006).
In the model, we used the basic electrophysiological parameters that were measured in larval zebrafish 4 days post-fertilization (Koyama et al., 2016) and kept them fixed for all simulations. We analyzed the effects of parameters of a linear transformation of the input, i.e. the slope and offset and furthermore the effects of noise on the input, on the initial condition, and on the spiking threshold. All parameters are listed in table 1.
effects:

- effects of increasing m:
  - mean response distance: mean increases linearly independent of threshold noise (only for high threshold noise slightly sub-linear)
  - variance of response distance: increases linearly for small threshold noise (except for a high lv value and low threshold noise, this is due to a very low mean and outliers that distort the standard deviation estimate), increases sub-linearly for medium threshold noise, slightly decreases for high threshold noise
  - mean response angle: decreases exponentially independent of threshold noise
  - variance of response angle: slightly decreases independent of threshold noise
  - mean time to collision: absolute value increases linearly independent of threshold noise, decreases more strongly for higher L/V values
  - variance of time to collision: very small increases for L/V values smaller than 0.9, for L/V values above 0.9 the variance is in general higher, for small threshold noise it is smallest for medium m-values and for higher threshold noise it also increases with m
  - mean response time: very similar to TTC
- effects of increasing threshold noise:
  - mean response distance:

Parameter	**Value (unit)**	**Comment**
E_L	-79 mV	Resting potential
R_M	10 MOhm	Membrane resistance
τ_m	23 ms	Membrane time constant
V_t	-61 mV	Mean spiking threshold
dt	0.001 s	Integration time step
T	5 s	Total time
sd_{thr}	1 mV	Standard deviation of spiking threshold noise
sd_I	5 mV	Standard deviation of input noise
sd_{init}	1 mV	Standard deviation of initial condition noise
m	1 °/s	Slope of linear transformation
b	0 °	Offset of linear transformation

Table 1 – Parameters of the single LIF neuron model with a looming stimulus input. Parameters that were explored are indicated either by a value range such as e.g. for μ_s or by a set with all explored values inside of curly brackets such as e.g. for σ_s.

- Effect of input transformation

- Effect of different noise sources
- Effect of input type

3.2. Input

-

3.3. Feedforward inhibition

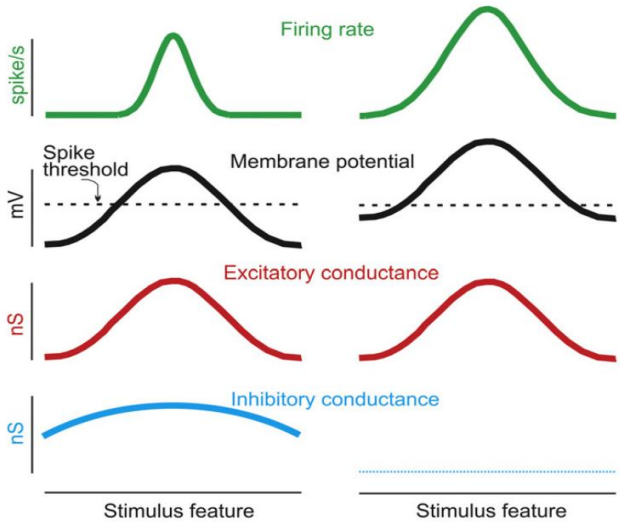

Figure 4. Inhibition Sharpens Stimulus Selective Spike Output via the "Iceberg Effect"
Schematic illustrates hypothetical tuning curves for firing rate (green), membrane potential (black), excitatory (red), and inhibitory (blue) conductances of a cortical neuron to stimulus features (e.g., orientation). Action potential firing occurs only when membrane potential exceeds a fixed spike threshold (dotted line). Responses are shown in the presence (left) and absence (right) of a weakly tuned inhibitory conductance. Inhibition leads to more narrowly tuned spike output by allowing only the strongest (preferred) excitatory stimuli to drive the membrane potential above spike threshold.

Figure 1 – how input sharpens tuning. From Isaacson and Scanziani (2011)

-

3.4. Cross-inhibition

-

3.5. Feedback inhibition

-

4. Discussion

- we focus here on the experimental results from Bhattacharyya et al. (2017) but one should keep in mind that their results might be specific to properties of experiment such as fish handling, fish age, species, arena, environment, stimulus setup (projection on screen)

References

K. Bhattacharyya, D. L. McLean, and M. A. MacIver. Visual threat assessment and reticulospinal encoding of calibrated responses in larval zebrafish. Current Biology, 27 (18):2751 – 2762.e6, 2017. ISSN 0960-9822. doi:10.1016/j.cub.2017.08.012. URL http://www.sciencedirect.com/science/article/pii/S0960982217310217.

T. Dunn, C. Gebhardt, E. Naumann, C. Riegler, M. Ahrens, F. Engert, and F. Del Bene. Neural circuits underlying visually evoked escapes in larval zebrafish. Neuron, 89(3): 613 – 628, 2016. ISSN 0896-6273. doi:10.1016/j.neuron.2015.12.021. URL http://www.sciencedirect.com/science/article/pii/S089662731501123X.

J. Isaacson and M. Scanziani. How inhibition shapes cortical activity. 72(2):231–243, 2011. ISSN 0896-6273. doi:10.1016/j.neuron.2011.09.027. URL http://www.sciencedirect.com/science/article/pii/S0896627311008798.

M. Koyama, F. Minale, J. Shum, N. Nishimura, C. B. Schaffer, and J. R. Fetcho. A circuit motif in the zebrafish hindbrain for a two alternative behavioral choice to turn left or right. ELIFE, 5, AUG 9 2016. ISSN 2050-084X. doi:10.7554/elife.16808.

D. Pita, B. A. Moore, L. P. Tyrrell, and E. FernÃąndez-Juricic. Vision in two cyprinid fish: implications for collective behavior. PeerJ, 3:e1113, Aug. 2015. ISSN 2167-8359. doi:10.7717/peerj.1113. URL https://doi.org/10.7717/peerj.1113.

T. Preuss and D. S. Faber. Central cellular mechanisms underlying temperature-dependent changes in the goldfish startle-escape behavior. Journal of Neuroscience, 23(13):5617–5626, 2003. ISSN 0270-6474. URL http://www.jneurosci.org/content/23/13/5617.

T. Preuss, P. E. Osei-Bonsu, S. A. Weiss, C. Wang, and D. S. Faber. Neural representation of object approach in a decision-making motor circuit. Journal of Neuroscience, 26 (13):3454–3464, 2006. ISSN 0270-6474. doi:10.1523/JNEUROSCI.5259-05.2006. URL http://www.jneurosci.org/content/26/13/3454.

S. B. Rosenthal, C. R. Twomey, A. T. Hartnett, H. S. Wu, and I. D. Couzin. Revealing the hidden networks of interaction in mobile animal groups allows prediction of complex behavioral contagion. Proceedings of the National Academy of Sciences of the United States of America, 112:4690–4695, Apr. 2015. ISSN 1091-6490. doi:10.1073/pnas.1420068112.

I. Temizer, J. Donovan, H. Baier, and J. Semmelhack. A visual pathway for looming-evoked escape in larval zebrafish. Current Biology, 25(14):1823 – 1834, 2015. ISSN 0960-9822. doi:10.1016/j.cub.2015.06.002. URL http://www.sciencedirect.com/science/article/pii/S0960982215006673.

E. D. Tytell and G. V. Lauder. Hydrodynamics of the escape response in bluegill sunfish, lepomis macrochirus. Journal of Experimental Biology, 211(21):3359–3369, 2008. ISSN 0022-0949. doi:10.1242/jeb.020917. URL http://jeb.biologists.org/content/211/21/3359.

A. Appendix